Research Square

Preprints are preliminary reports that have not undergone peer review.
They should not be considered conclusive, used to inform clinical practice,
or referenced by the media as validated information.

Global agricultural shocks from Atlantic overturning collapse

Rebecca Frank

rebecca@allfed.info

Alliance to Feed the Earth in Disasters (ALLFED) https://orcid.org/0009-0005-2086-3131

Michael Hinge

Alliance to Feed the Earth in Disasters (ALLFED)

Simon Blouin

Alliance to Feed the Earth in Disasters (ALLFED)

Florian Jehn

Alliance to Feed the Earth in Disasters (ALLFED) https://orcid.org/0000-0002-7296-8008

Emma Comerford

Alliance to Feed the Earth in Disasters (ALLFED)

Mahi Shah

Alliance to Feed the Earth in Disasters (ALLFED)

Sebasstián Adriano Heredia

Alliance to Feed the Earth in Disasters (ALLFED)

David Denkenberger

Alliance to Feed the Earth in Disasters (ALLFED)

Physical Sciences - Article

Keywords:

Posted Date: August 27th, 2026

DOI: https://doi.org/10.21203/rs.3.rs-10243822/v1

License: This work is licensed under a Creative Commons Attribution 4.0 International License.
Read Full License

Additional Declarations: There is **NO** Competing Interest.

Global agricultural shocks from Atlantic overturning collapse

Rebecca Frank [a,*], Michael Hinge[a], Simon Blouin[a], Florian Ulrich Jehn[a, b, c, d], Emma Comerford[a], Mahi Shah[a], Sebasstián Adriano Heredia[a], David C. Denkenberger [a,e]

Affiliations:

[a] Alliance to Feed the Earth in Disasters (ALLFED), 603 S. Public Rd #57 Lafayette, CO 80026, USA.

[b]Center for Critical Computational Studies (C³S), Goethe University Frankfurt, Frankfurt am Main, Germany

[c] Societal Dynamics (SoDy), Toronto, Canada

[d] Institute for International Legal Relations, FernUniversität in Hagen, Germany

[e] Department of Mechanical Engineering, University of Canterbury, Christchurch, New Zealand

*Corresponding author: Rebecca Frank, rebecca@allfed.info.

The Atlantic Meridional Overturning Circulation (AMOC) functions as a critical climate tipping element, potentially capable of abrupt collapse under sustained anthropogenic forcing [1,2]. Current agricultural impact assessments predominantly focus on ongoing climate change trajectories [3,4], leaving the global food system's vulnerability to a climate shock like an AMOC collapse unquantified. Here we show the global agricultural and economic consequences of such a collapse. By coupling a 100-year climate anomaly [5] with global crop simulations, we identify a 5.3% structural decline in global wheat, maize, and rice production. We demonstrate that this biophysical penalty is geographically asymmetrical, triggering production collapses of 12% to 19% across highly concentrated Northern Hemisphere export hubs. Superimposing these reductions onto current global food trade networks reveals severe structural dietary deficits in import-dependent nations [6]. Finally, economic modeling

indicates that if this protracted multi-breadbasket failure outpaces market adaptation, global cereal prices could structurally spike by up to 40%. These findings provide a replicable pipeline from climate tipping points to human impact, underscoring the urgent necessity of preemptive, climate-resilient food infrastructure.

1. Introduction

The Atlantic Meridional Overturning Circulation (AMOC) is a critical component of the Earth's climate system, capable of abrupt weakening or complete collapse under sustained anthropogenic forcing and freshwater influx from the melting Greenland Ice Sheet [1,2,7]. The climatological consequences of such a collapse include severe Northern Hemisphere cooling, the southward shifting of the Intertropical Convergence Zone (ITCZ), extreme weather volatility, and the profound disruption of monsoon systems [8–10].

Current agricultural impact assessments predominantly focus on gradual climate change scenarios, simulating linear temperature increases and altered precipitation patterns [3,4]. However, the global food system is highly optimized for the climatic stability of the Holocene and is uniquely vulnerable to non-linear tipping points like an AMOC collapse, which falls entirely outside the parameters of gradual warming models [11].

While occasionally mischaracterized as an instantaneous event, an AMOC collapse is a protracted biophysical transition; the resulting climate anomalies would materialize gradually over several decades, fundamentally altering the baseline of global agriculture. Existing literature on these agricultural impacts has largely been confined to regional analyses or high-level macro-ecological baselines [12–15]. The interconnected nature of the global food system necessitates a spatially explicit,

47 macro-level understanding of how a structural transition to a new climate state would shock total
48 and regional calorie production.

49 To address this gap, this paper provides the first quantified, global assessment of crop yield and
50 calorie production shocks resulting from an AMOC collapse. By coupling a 100-year AMOC-
51 collapse climate anomaly with a global gridded crop model, we isolate the biophysical yield shock
52 on key staple crops (wheat, maize, and rice). We subsequently analyze the propagation of these
53 yield reductions through international trade networks to identify resultant price pressures and
54 assess the scale of resilient food adaptations required to maintain global calorie sufficiency.

55 # 2. Results

56 ## 2.1 Global crop yield reductions after AMOC collapse

57 Applying the AMOC collapse climate anomaly under a precipitation-scaled irrigation scenario
58 results in a 5.3% decline in global caloric production averaged across wheat, maize, and rice
59 (Figure 1). Changes to crop yield volatility could not be isolated with statistical confidence, as the
60 single 100-year climate trajectory provides insufficient data to distinguish genuine shifts from
61 inter-annual noise or capture intra-monthly weather extremes.

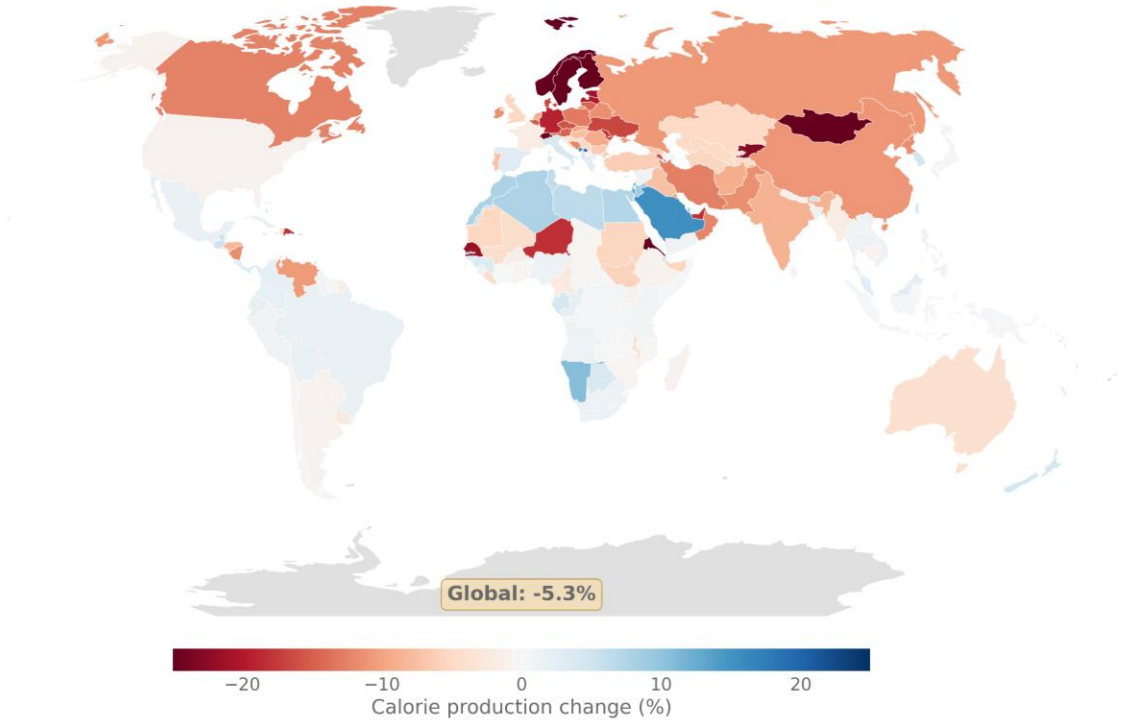


Figure 1: Projected global caloric yield anomalies under a Precipitation-Scaled Irrigation scenario following an AMOC collapse. *This primary biophysical assessment maps the spatial distribution of yield changes across major caloric staples (maize, wheat, and rice) utilizing the HadGEM3-GC3.1-MM climate anomaly. The model assumes the yield benefit of existing irrigation infrastructure is reduced proportionally to grid-cell-level precipitation declines. The aggregate global caloric production falls by 5.3%.*

2.2 Food trade disruption after AMOC collapse

The propagation of AMOC-driven yield shocks through the global food trade network reveals asymmetrical vulnerabilities. Crucially, this static network analysis assumes that national exports scale down proportionally to production declines. In reality, nations inherently prioritize domestic consumption and often only export excess supply; therefore, this proportional scaling represents a conservative baseline, and the actual contraction of available global export volumes could be more severe. When mapping these baseline supply contractions against national dietary reliance (import

loss as a percentage of domestic consumption), severe exposure is dictated by structural import dependence rather than broad hemispheric divides, heavily impacting regions across Africa, Asia, the Middle East, and Europe.

Specifically, wheat presents the most severe dietary vulnerabilities, heavily concentrated in structurally import-dependent tropical nations and climate-stressed importers (Figure 2). Global dietary exposure to maize and rice import deficits remains broadly negligible, with structural vulnerabilities acutely isolated to specific high-reliance import markets across Europe, Africa, the Middle East, and Central Asia (Figures 3 and 4).

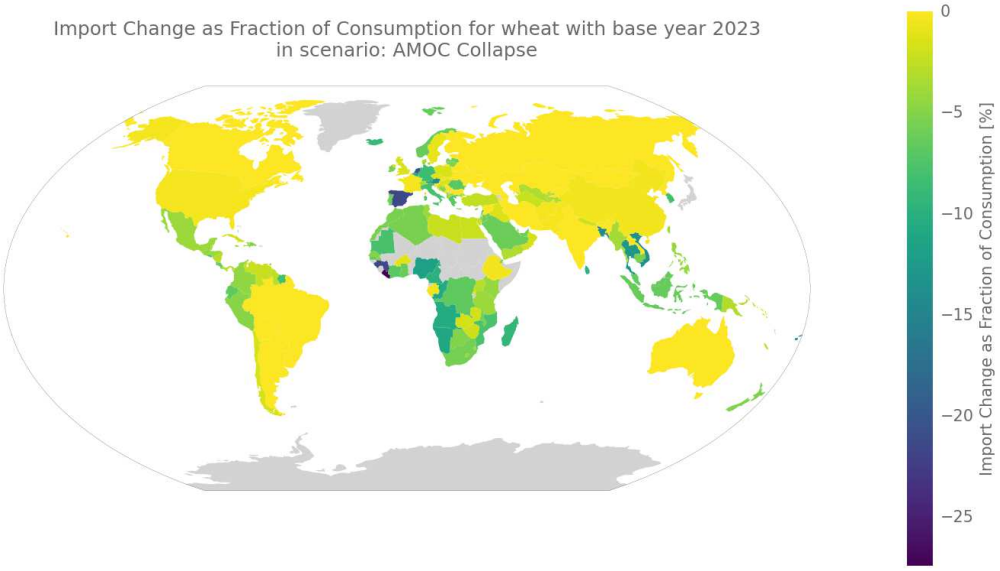


Figure 2: Projected dietary exposure to wheat import deficits following an AMOC collapse. *This network trade analysis maps the structural reduction in wheat imports relative to each nation's baseline domestic consumption (FAO Food Balance Sheets, base year 2023). Assuming a proportional scaling of export volumes relative to domestic yield shocks, the most severe dietary vulnerabilities are concentrated in structurally import-dependent tropical nations (e.g., Guinea, Liberia, Thailand) and climate-stressed importers (e.g., Spain). Conversely, major global producers experience minimal relative domestic dietary disruption.*

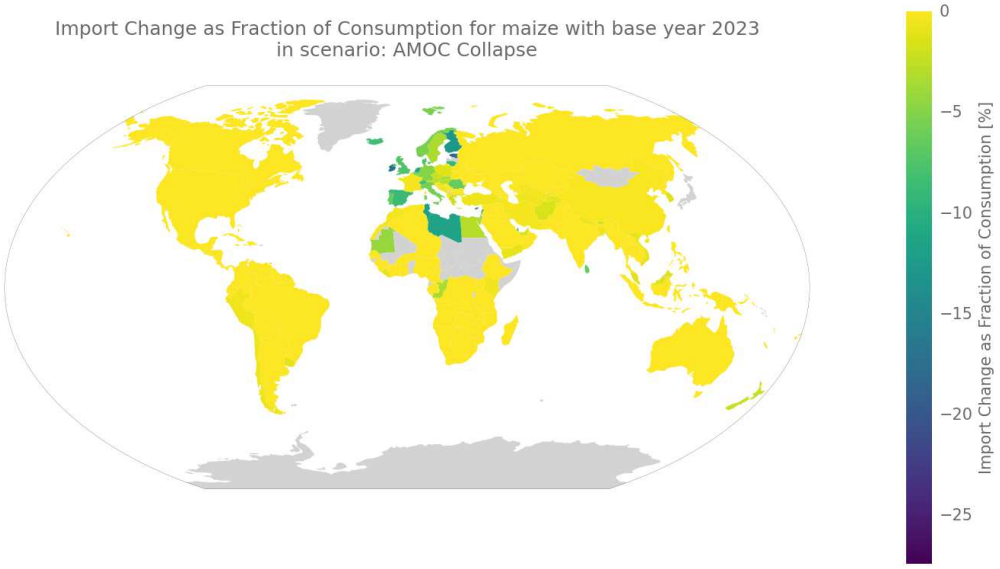


Figure 3: Projected dietary exposure to maize import deficits following an AMOC collapse. *This network trade analysis maps the structural reduction in maize imports relative to baseline domestic consumption (FAO Food Balance Sheets, base year 2023). Global dietary exposure remains broadly negligible, with disruptions highly isolated to specific import-reliant markets. The most significant consumption risks are concentrated across the majority of Europe—excluding self-sufficient producers such as France—and specific North African nations, notably Libya, Egypt, and Mauritania.*

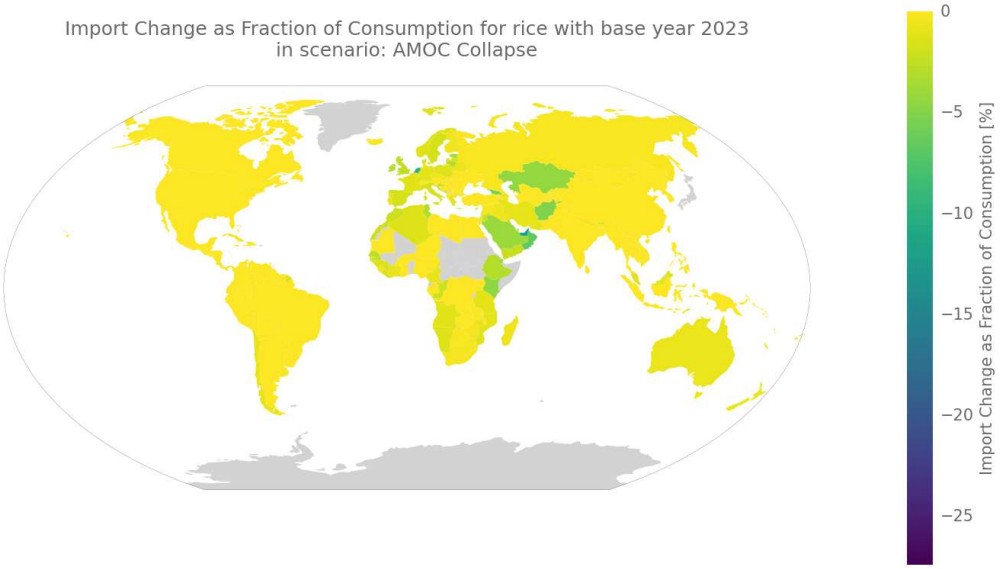


Figure 4: Projected dietary exposure to rice import deficits following an AMOC collapse. *This network trade analysis maps the structural reduction in rice imports relative to each nation's baseline domestic consumption (FAO Food Balance Sheets, base year 2023). While global dietary exposure remains broadly negligible, notable structural deficits are isolated to highly dependent import markets, specifically Kazakhstan, Afghanistan, Kenya, Ethiopia, and the Middle East.*

2.3 Economic impacts

The 5.3% yield shock translates into structurally higher global pricing, heavily dependent on the speed of market adaptation. Under pessimistic short-run supply elasticity assumptions [16], this unadapted deficit could drive a global cereal price spike of up to 40% above baseline levels. Conversely, if long-run market elasticity is achieved—where farmers have the time to expand cultivated areas, increase farming intensity, and shift feed and biofuel crops toward human consumption [17]—the structural 5.3% yield deficit would result in a sustained, long-term price increase of approximately 17.5%.

3. Discussion

3.1 Implications of crop yield reductions

The crop modeling demonstrates a 5.3% decline in global caloric production for major staples under the primary precipitation-scaled irrigation scenario. This global aggregate represents a baseline shift that materializes gradually over several decades as the AMOC shutdown fully expresses. However, this targeted agricultural penalty aligns remarkably well with established macro-ecological projections; notably, early coupled climate models estimated a roughly 5% decline in global terrestrial net primary productivity (NPP) during the initial decades of an AMOC

collapse [15]. Despite differing temporal trajectories between the models, the climate anomalies driving these vegetation losses are highly comparable. Vellinga and Wood modeled an average 1.4°C cooling in the Northern Hemisphere to reach their 5% terrestrial NPP deficit, which closely mirrors the 2.0°C Northern Hemisphere cooling and resulting 5.3% cereal deficit modeled in our scenario.

While this global aggregate may initially appear moderate, it obscures critical regional production failures. The biophysical shock disproportionately penalizes the Northern Hemisphere, driving a severe relative collapse approaching 40% in marginal northern agricultural zones (e.g., Scandinavia). More critically for global food security, the ensuing thermo-hydrological shock geographically aligns with several of the world's most concentrated and high-yielding agricultural hubs. This drives localized production failures of roughly 16% to 19% across major European breadbaskets (such as Germany and Ukraine) and a 12.4% structural decline in Canada. Consequently, the burden of the biophysical shock is highly asymmetrical, damaging the export capacity for much of the Northern Hemisphere and fracturing the foundational supply lines of the global food system.

3.2 The multiplier effect of trade protectionism

The projected price increases above assume a cooperative global market. In reality, historical supply deficits consistently trigger reactionary trade protectionism, as governments implement export bans to shield domestic consumers from inflation [18,19]. This has created a cascading multiplier effect in previous yield shocks, that artificially contracts global supply and further inflates prices. For instance, uncooperative trade policies accounted for roughly half of the 90% rice price surge during the 2008–2011 crisis [19] and artificially inflated world wheat prices by up to

67% during the 2022 supply shock [20]. This protectionism extends to critical inputs, as seen when 2022 export quotas on fertilizers removed 15% of global supply and severely compounded price shocks [21,22].

Under an AMOC collapse, the 5.3% biophysical yield deficit could trigger domestic inflation thresholds across major exporters, especially in scenarios where countries are slow to adapt or initially fail to realize a collapse is underway, sparking a wave of cascading restrictions. Predictive models suggest this uncooperative scenario could slash global food export supply by ~21% [23]. Therefore, the raw caloric deficit represents only the baseline hazard; the ultimate shock to global food affordability may be severely multiplied by the rapid fragmentation of the global trade network.

3.3 Unadapted hazard vs. long-term elasticity

When evaluating the trade disruptions modeled in Section 2.2, it is critical to distinguish between the immediate, unadapted hazard and the long-term reality of market elasticity. The static network analysis quantifies the "adaptation deficit"—the raw structural void that occurs if production and trade topologies remain frozen. While the AMOC collapse is a multi-decadal transition, mapping this unadapted scenario is crucial for policymakers; it isolates the exact magnitude of the shock that would hit the current agricultural architecture if governments and markets fail to proactively react.

For example, the model indicates severe structural wheat deficits for highly exposed markets such as Spain, Guinea, and Liberia, driven by the severe production failures of their primary Northern Hemisphere export partners. Over a multi-decadal time frame, extreme price signals would force these highly dependent nations to restructure trade partnerships and source novel origins.

Simultaneously, major agricultural exporters retaining baseline capacities would shift production geographically to capitalize on new comparative advantages, dynamically altering export volumes.

These static vulnerabilities represent the sheer magnitude of the frictional challenge the global food system must overcome. Market fungibility and production shifts will organically resolve portions of this deficit, but the transition will carry immense financial and developmental costs for nations lacking the capital to outbid competitors in a structurally constrained global market.

3.4 Adaptations required for global calorie sufficiency

Adapting to an AMOC collapse cannot rely solely on the geographical relocation of conventional agriculture, as this would trigger a secondary ecological catastrophe. Even under baseline climate conditions, the global food system is projected to require 2 to 10 million square kilometers of new agricultural land by 2050 to meet growing dietary demands—an expansion projected to encroach on the habitats of roughly 88% of terrestrial vertebrate species, largely driving the conversion of existing wild and grazing lands [24].

An AMOC collapse would compound this existing pressure. While only a negligible fraction of global staple cropland falls below a strict non-viability threshold (500 kg/ha/yr) following the collapse, the severe yield degradation across highly productive northern arable land would force an accelerated displacement of agricultural production into surviving tropical and Southern Hemisphere biomes. This structural spatial restructuring would vastly accelerate deforestation, transforming a climate tipping point into a biodiversity crisis. Consequently, adaptation necessitates a broad portfolio of climate-resilient, land-efficient interventions, such as redirecting feed and biofuels to human consumption, scaling greenhouses [25], crop relocation [26] and expanding planted areas strictly onto non-virgin lands. This must be deployed alongside climate-decoupled

"resilient foods" (e.g., single-cell proteins, leaf protein concentrate, cellulosic sugar, and seaweed cultivation) to fill the structural caloric void while reducing conversion pressure on natural ecosystems [27,28].

3.5 Price dynamics and food affordability

The ultimate price impact of an AMOC collapse will depend heavily on the ability of global agricultural supply and demand to adapt to the altered yield environment. If the biophysical shock were to outpace adaptation, the economic impacts could be severe, driving a short-term global price spike of up to 40% above baseline levels. However, if more optimistic values for long-run elasticity apply, and farmers can significantly alter their planting patterns and input usage, the structural 5.3% yield deficit could result in a sustained, long-term price increase of approximately 17.5%.

Based on current World Bank estimates of poverty and income distribution [29], a sustained price increase within this range threatens to push between 30 million and 340 million additional people into food poverty. Crucially, these estimates only refer to the AMOC hazard in isolation; the true pressure on food affordability will interact dynamically with baseline population growth, shifting dietary demands, and the compounding disruptions of conventional anthropogenic climate change. Furthermore, demand policy could intervene to reduce the pressure if human consumption is prioritized and animal feed or biofuel uses are reduced at the margin.

3.6 Interactions with existing climate change trends

An AMOC collapse will not manifest in isolation; its impacts will compound with the baseline anthropogenic warming trajectory that triggered it. First, the collapse is projected to significantly

reduce precipitation across much of the Northern Hemisphere [9], exacerbating existing water scarcity and compounding the projected reversion of millions of hectares of irrigated cropland to rainfed management [30]. This will be particularly acute in the Indian subcontinent and MENA regions where water access is already critically threatened [31]. Compensating through enhanced groundwater extraction risks accelerating the depletion of non-renewable aquifers.

Second, the collapse fundamentally alters the geographical expectations for future agricultural viability. Under baseline warming projections, rising temperatures are expected to improve farming conditions and expand arable frontiers across Eastern Europe, Central Asia, and parts of Siberia [32–35]. An AMOC collapse could sharply reverse this trajectory, forcing sharp yield declines across these anticipated regional breadbaskets and eliminating the expected high-latitude adaptation buffer.

3.7 Sensitivity to Climate Model Selection and Cooling Severity

The magnitude of the projected agricultural deficit is highly contingent upon the specific climate forcing data applied. The structural deficits modeled in this study should be interpreted strictly within the parameters of the HadGEM3 forcing which represents only one possible trajectory within a spectrum of climate models. Recent high-resolution simulations [2] project significantly sharper and more rapid temperature declines, with localized cooling over Europe and the Northern Hemisphere progressing at rates exceeding 3°C per decade. A more severe cooling trajectory could rapidly expand the geographical footprint of non-viable arable land, potentially increasing the 5.3% aggregate production collapse. However, the coupled climate-crop framework established here provides a scalable pipeline for future meta-analyses to ingest divergent climate datasets.

3.8 Limitations and Recommendations for Future Research

Recent evaluations of global gridded crop models indicate a systemic tendency to underestimate crop yield losses during extreme weather events, particularly under conditions of excessive rainfall and compound heat-drought extremes [36]. Consequently, the unadapted biophysical baseline of a 5.3% global caloric reduction likely represents a cautious estimate.

Future research should expand to incorporate additional commodities (e.g., soy), multi-cropping systems, and secondary Earth system tipping cascades (e.g., Amazon dieback) that would trigger massive secondary agricultural shocks [37]. Subsequent modeling should also utilize a +2°C "adapted" crop baseline to evaluate the feasibility of physical and economic adaptations over the next 100 years. Additionally, the static trade network should be coupled with a computable general equilibrium (CGE) model to capture economic elasticity, dynamic trade rerouting, and the multiplier effect of reactionary export bans. Finally, future work should rigorously quantify the capacity of targeted interventions—such as resilient foods and waste reduction—to close residual calorie gaps without triggering unintended maladaptive ecological consequences.

4. Conclusion

This analysis quantifies the global food system's unadapted baseline vulnerability to an AMOC collapse. Crucially, these findings do not represent a definitive forecast of the crisis; rather, the coupled climate-crop framework presented here serves as a foundational methodology to be built upon in future research utilizing alternative climate ensembles. While the projected 5.3% reduction in global caloric production appears moderate in aggregate, it obscures acute structural deficits caused by the severe disruption of highly concentrated Northern Hemisphere export hubs.

Rather than predicting an inevitable outcome, these static models define the magnitude of the global adaptation deficit. Over a multi-decadal timeline, markets will inevitably adapt through geographic crop relocation, demand elasticity, and the restructuring of trade networks. However, closing this massive structural void using traditional agricultural expansion risks catastrophic global biodiversity loss, and historical precedents suggest the economic transition will be highly volatile. Mitigating this systemic shock therefore requires preemptive global interventions and a paradigm shift toward resilient, land-efficient caloric infrastructure.

References

1. Armstrong McKay, D. I. *et al.* Exceeding 1.5°C global warming could trigger multiple climate tipping points. *Science* **377**, eabn7950 (2022).

2. van Westen, R. M., Kliphuis, M. & Dijkstra, H. A. Physics-based early warning signal shows that AMOC is on tipping course. *Sci. Adv.* **10**, eadk1189 (2024).

3. Rosenzweig, C. *et al.* Assessing agricultural risks of climate change in the 21st century in a global gridded crop model intercomparison. *Proc. Natl. Acad. Sci.* **111**, 3268–3273 (2014).

4. Müller, C. *et al.* Global gridded crop model evaluation: benchmarking, skills, deficiencies and implications. *Geosci. Model Dev.* **10**, 1403–1422 (2017).

5. Bathiany, S., Patrizio, C., Ferreira, L. & Jackson, L. ClimTip ESM simulations D7.1 & D8.1 - monthly data. Zenodo https://doi.org/10.5281/zenodo.16784934 (2025).

6. Jehn, F. U. *et al.* Food trade disruption after global catastrophes. *Earth Syst. Dyn.* **16**, 1585–1603 (2025).

7. Srokosz, M. A. & Bryden, H. L. Observing the Atlantic Meridional Overturning Circulation yields a decade of inevitable surprises. *Science* **348**, 1255575 (2015).

8. Ben-Yami, M. *et al.* Impacts of AMOC Collapse on Monsoon Rainfall: A Multi-Model Comparison. *Earths Future* **12**, e2023EF003959 (2024).

9. Jackson, L. C. *et al.* Global and European climate impacts of a slowdown of the AMOC in a high resolution GCM. *Clim. Dyn.* **45**, 3299–3316 (2015).

10. Bellomo, K. *et al.* Impacts of a weakened AMOC on precipitation over the Euro-Atlantic region in the EC-Earth3 climate model. *Clim. Dyn.* **61**, 3397–3416 (2023).

11. Gaupp, F., Hall, J., Hochrainer-Stigler, S. & Dadson, S. Changing risks of simultaneous global breadbasket failure. *Nat. Clim. Change* **10**, 54–57 (2020).

12. Ritchie, P. D. L. *et al.* Shifts in national land use and food production in Great Britain after a climate tipping point. *Nat. Food* **1**, 76–83 (2020).

13. Mirow, J. Expert insights into the health and societal risks of a potential AMOC collapse in Europe: Focus on Germany. *PLOS Clim.* **5**, e0000735 (2026).

14. OECD. *Managing Climate Risks, Facing up to Losses and Damages: Understanding, Reducing and Managing Risks*. (OECD Publishing, 2021). doi:10.1787/55ea1cc9-en.

15. Vellinga, M. & Wood, R. A. Global Climatic Impacts of a Collapse of the Atlantic Thermohaline Circulation. *Clim. Change* **54**, 251–267 (2002).

17. Peterson, W. International Supply Response. *Agric. Econ.* **2**, 365–374 (1988).

18. Mamun, A. & Laborde, D. Role of International Price and Domestic Inflation in Triggering Export Restrictions on Food Commodities. *Agric. Econ.* **56**, 905–923 (2025).

19. Martin, W. & Anderson, K. Export Restrictions and Price Insulation During Commodity Price Booms. *Am. J. Agric. Econ.* **94**, 422–427 (2012).

20. Tripathi, A. K. & Mishra, A. K. Wheat Export Restriction and Effects on India's Domestic Prices: A Nonlinear ARDL Modeling Approach. *J. Agric. Resour. Econ.* https://doi.org/10.22004/ag.econ.349179 (2025) doi:10.22004/ag.econ.349179.

21. USDA. Impacts and Repercussions of Price Increases on the Global Fertilizer Market | USDA Foreign Agricultural Service. https://www.fas.usda.gov/data/impacts-and-repercussions-price-increases-global-fertilizer-market (2022).

22. Vos, R., Glauber, J., Hebebrand, C. & Rice, B. Global shocks to fertilizer markets: Impacts on prices, demand and farm profitability. *Food Policy* **133**, 102790 (2025).

23. Espitia, A., Rocha, N. & Ruta, M. *Covid-19 and Food Protectionism: The Impact of the Pandemic and Export Restrictions on World Food Markets*. (World Bank, Washington, DC, 2020). doi:10.1596/1813-9450-9253.

24. Williams, D. R. *et al.* Proactive conservation to prevent habitat losses to agricultural expansion. *Nat. Sustain.* **4**, 314–322 (2021).

25. Alvarado, K. A., Mill, A., Pearce, J. M., Vocaet, A. & Denkenberger, D. Scaling of greenhouse crop production in low sunlight scenarios. *Sci. Total Environ.* **707**, 136012 (2020).

26. Blouin, S. *et al.* Strategic crop relocation could substantially mitigate nuclear winter. *ALLFED - Alliance to Feed the Earth in Disasters* https://allfed.info/research/publications-and-reports/pre-print/crop-relocation-nuclear-winter (2025).

27. García Martínez, J. B., Behr, J. & Denkenberger, D. C. Food without agriculture: Food from CO2, biomass and hydrocarbons to secure humanity's food supply against global catastrophe. *Trends Food Sci. Technol.* **150**, 104609 (2024).

28. García Martínez, J. B., Behr, J., Pearce, J. & Denkenberger, D. Resilient foods for preventing global famine: a review of food supply interventions for global catastrophic food shocks including nuclear winter and infrastructure collapse. *Crit. Rev. Food Sci. Nutr.* **65**, 6068–6094 (2025).

29. The World Bank. Poverty and Inequality Platform. https://pip.worldbank.org/ (2026).

30. Elliott, J., Deryng, D. & Wisser, D. Constraints and potentials of future irrigation water availability on agricultural production under climate change. https://www.pnas.org/doi/10.1073/pnas.1222474110 (2013) doi:10.1073/pnas.1222474110.

31. Wassenburg, J. A. *et al.* Penultimate deglaciation Asian monsoon response to North Atlantic circulation collapse. *Nat. Geosci.* **14**, 937–941 (2021).

32. Belyaeva, M. & Bokusheva, R. Will climate change benefit or hurt Russian grain production? A statistical evidence from a panel approach. *Clim. Change* **149**, 1–13 (2018).

33. Sirotenko, O., Abashina, H. & Pavlova, V. Sensitivity of the Russian agriculture to changes in climate, CO2 and tropospheric ozone concentrations and soil fertility. *Clim. Change* **36**, 217–232 (1997).

34. Gordeev, R. V., Pyzhev, A. I. & Zander, E. V. Does Climate Change Influence Russian Agriculture? Evidence from Panel Data Analysis. *Sustainability* **14**, 718 (2022).

35. Kiselev, S., Romashkin, R., Nelson, G., Mason-D'Croz, D. & Palazzo, A. Russia's Food Security and Climate Change: Looking into the Future. *Econ. Open-Access Open-Assess. E-J.* **7**, (2013).

36. Auer, C. *et al.* Global gridded crop models underestimate yield losses from climatic extremes. Preprint at https://doi.org/10.21203/rs.3.rs-7181139/v1 (2026).

37. Flores, B. M. *et al.* Critical transitions in the Amazon forest system. *Nature* **626**, 555–564 (2024).

5. Methods

5.1 Climate scenarios

To isolate the biophysical shock of an AMOC collapse, we constructed a 100-year climate dataset. Global climate models cannot be used directly, as they contain systematic biases in absolute weather values. Instead, we started from observed daily weather. We use the NASA POWER record [38] for the years 2001–2020, looped five times to fill the 100-year window (data prior to 2001 was excluded to avoid superimposing a historical warming trend onto the AMOC shock). We then offset this baseline using monthly change factors derived from HadGEM3-GC3.1-MM control and AMOC-collapse simulations [5].

This forcing applies a moderate regional cooling trajectory, characterized by localized temperature declines of 3°C to 5°C across key Northern Hemisphere latitudes (e.g., London and Reykjavik). This establishes the unadapted biophysical penalty applied to the crop models. Notably, this represents a less severe temperature shock compared to other recent AMOC collapse simulations, which project localized temperature drops of 7°C to 13°C for the same regions [2]. A discussion on the sensitivity of our baseline to these divergent climate models is provided in Section 3.7.

However, the derived change factors could not be applied to the baseline in raw form. Doing so would stack the climate model's internal noise on top of the observed weather's natural variability, artificially inflating variance. We therefore smoothed the monthly change factors with a LOESS (locally estimated scatterplot smoothing) filter (bandwidth fraction = 0.3) at each grid cell, retaining the forced trajectory of the AMOC collapse while removing interannual noise. The smoothed deltas were then applied to the baseline to produce the final perturbed climate series.

5.2 Crop modeling framework

Crop yield simulations were conducted utilizing the Mink global gridded crop modeling system, which is built on version 4.7 of the Decision Support System for Agrotechnology Transfer (DSSAT) framework [26,39]. As a process-based model, Mink simulates crop growth through mechanistic representations of photosynthesis, respiration, phenology, and water and nutrient dynamics. Simulations were conducted at the climate data 0.56° × 0.83° (latitude × longitude) spatial resolution. Soil properties were derived from the global SoilGrids database [40], while current crop distributions and irrigated versus rainfed classifications were established using the SPAM 2020 datasets [41]. To strictly isolate the biophysical hazard of the climate shock, both global crop distribution and atmospheric CO2 concentrations were held constant at present-day levels, excluding the highly uncertain variables of future socio-economic adaptation or CO2 fertilization. Fertilizer application rates were also held constant at current levels based on FAO statistics [42].

For this first-pass assessment, we focused on three primary cereal caloric staples: maize, wheat, and rice, which collectively account for nearly half of all dietary calories consumed globally and constitute the foundation of international food security [43]. The current Mink framework configuration simulates a single harvest per year for all crops. Consequently, planting dates were optimized to maximize yield for this single primary harvest by simulating each crop across twelve possible planting months and selecting the month yielding the highest output. In regions characterized by both a dry and a monsoon season, the model algorithm naturally selects the monsoon season when water limitations are the binding constraint. While this provides a robust baseline for the primary growing season, it acts as a conservative estimate for total caloric loss. This limitation is particularly relevant for global rice production, which relies heavily on multiple cropping in major Asian breadbaskets. The model captures the yield decline from the lack of

supplemental rainfall during the primary wet season, but does not capture the potential failure of secondary or tertiary rice harvests during less irrigated dry seasons.

5.3 Simulation Scenarios

A critical methodological challenge in climate anomaly modeling is the handling of global irrigation systems. To establish a realistic baseline for downstream trade and economic analyses, we utilized a Precipitation-Scaled Irrigation scenario. This model assumes the yield boost provided by irrigation is reduced proportionally to the grid-cell-level decline in precipitation. This approach serves as an approximate middle path; it likely underestimates total crop failures in regions reliant on complex double-cropping, while conversely overstating the immediate vulnerability of agricultural systems buffered by deep groundwater aquifers, which remain partially insulated from precipitation shocks.

To establish rigorous analytical bounds for this primary methodology, two extreme sensitivity scenarios were evaluated:

Optimistic Bound (full irrigation): This parameter assumes current global irrigation applications continue unabated despite the severe hydrological deficits introduced by an AMOC collapse, effectively isolating the modeled crops from the precipitation deficit (see Extended Data Figure 1).

Pessimistic Bound (no irrigation): This parameter forces a complete failure of all global irrigation infrastructure, transitioning all agricultural grid cells to strictly rainfed conditions to evaluate the unmitigated compounding effects of the thermal and moisture shocks (see Extended Data Figure 2).

5.4 Food trade model

To quantify the systemic vulnerability of the global food system, we analyzed the propagation of the biophysical yield shock through the international food trade network via the pytradeshifts framework [6]. The global trade network is constructed as a weighted directed graph, where nodes represent countries and the weights of the edges represent bilateral trade volumes initialized with 2022 reference production and trade data from the FAO. To ensure the network reflects direct point-of-origin to point-of-destination trade movements, the model adjusts for and removes re-exports. Furthermore, to isolate the primary structural dependencies of the global food system, bilateral trade flows falling below the 75th percentile in trade volume were excluded from the initialization.

Crucially, this analysis does not attempt to forecast bilateral trade flows decades into the future, as long-term market elasticity, demographic shifts, and geopolitical realignments render such temporal projections highly uncertain. Instead, to maintain methodological consistency with our unadapted crop baseline, we utilized the present-day trade network as a static baseline stress test.

We mapped the current topology of the global food system using a complex network model. To determine post-catastrophe trade exposure, national exports were forced to decrease proportionally to the biophysical yield shock derived from the Precipitation-Scaled Irrigation scenario. The network topology does not introduce new trade connections to simulate unadapted conditions. By superimposing these gridded yield reductions onto the present-day network, we tracked how abrupt supply contractions propagate through central hub exporters. Because the overarching structure of trade communities remains stable under a yield shock of this specific magnitude, community rewiring metrics (such as the Jaccard distance) were not utilized. Ultimately, this approach isolates

invariant geographical vulnerabilities and quantifies the global "adaptation deficit"—the order-of-magnitude structural gap between the calories a collapsed-AMOC climate can provide and the calories the current human system requires. This metric establishes the required scale for future market adaptations, shifting trade partnerships, and resilient food deployments.

5.5 Economic modelling

To estimate the humanitarian impact of an AMOC collapse on global cereal prices and broad affordability, we ran a partial equilibrium model focusing exclusively on cereals, utilizing the framework of Hinge et al.[44]. The model translates a multi-year yield shock across the global cereal market into a price shock by simulating dynamic shifts in consumer, producer, and storage behavior. It operates as a surplus optimization problem across discrete crop-year time steps, where agents adjust production and storage decisions to maximize utility and profits based upon rational expectations of future yields and prices. Inventories link these discrete periods through arbitrage, subject to an assumed annual cost of carry of 7.6% of the prevailing cereal price.

Because supply elasticity—the degree to which a change in prices results in a corresponding expansion or contraction of crop output—varies significantly depending on warning time, baseline climate pressures, and regulatory constraints, differing studies yield divergent estimates [45,46]. To account for this uncertainty, the model evaluates the 5.3% biophysical yield deficit under two bounding elasticity scenarios, utilizing log-log functions for both supply and demand.

Pessimistic Bound (short-run elasticity): This scenario assumes farmers have limited information regarding the AMOC collapse, or that their capacity to raise output is heavily constrained by compounding climate pressures. Utilizing elasticity estimates for unexpected yield shocks [16], global cereal demand elasticity is set at -0.066 and supply elasticity at 0.097. To accurately capture

444 expectations and price variance, the model solves for the equilibrium by running a Monte Carlo
445 simulation of 10,000 random yield scenarios to find the point of minimum expected availability.
446 Under these constrained parameters, compounding the modeled 5.3% yield deficit establishes a
447 pessimistic upper bound, driving a global price spike of up to 40% above baseline levels.

448 Optimistic Bound (long-run elasticity): However, over the multi-decadal time frame of an AMOC
449 collapse, agricultural markets could exhibit significantly higher elasticity, reducing the shock.
450 Driven by sustained price rises and the need for more output, farmers and processors could expand
451 cultivated areas, increase farming intensity, and shift crops currently utilized for feed and biofuels
452 toward direct human consumption. The long-run elasticity of cereal supply has been estimated as
453 high as 1.19 [47], suggesting that with more time to respond (six years in the study). However,
454 estimates vary, and a more recent IMF estimate gives long run elasticity to be around 0.498 for a
455 basket of cereals [48]. If this long-run elasticity applies instead, and farmers can significantly alter
456 their planting patterns and input usage, the structural 5.3% yield deficit would result in a sustained,
457 long-term price increase of approximately 17.5%.

Methods References

38. Zhang, T. *et al.* A Global Perspective: NASA's Prediction of Worldwide Energy Resources (POWER) Project. in (London, United Kingdom, 2007).

39. Jones, J. W. *et al.* The DSSAT cropping system model. *Eur. J. Agron.* **18**, 235–265 (2003).

40. Han, E., Ines, A. V. M. & Koo, J. Development of a 10-km resolution global soil profile dataset for crop modeling applications. *Environ. Model. Softw.* **119**, 70–83 (2019).

41. Institute (IFPRI), I. F. P. R. Global Spatially-Disaggregated Crop Production Statistics Data for 2020 Version 2.0 Release 2. Harvard Dataverse https://doi.org/10.7910/DVN/SWPENT (2026).

42. Gbegbelegbe, S. *et al.* Baseline simulation for global wheat production with CIMMYT mega-environment specific cultivars. *Field Crops Res.* **202**, 122–135 (2017).

43. Erenstein, O., Jaleta, M., Sonder, K., Mottaleb, K. & Prasanna, B. M. Global maize production, consumption and trade: trends and R&D implications. *Food Secur.* **14**, 1295–1319 (2022).

44. Hinge, M. *et al.* Calculating equilibrium cereal prices during a multi-year productivity shock. (2026).

45. Hertel, T. W., Baldos, U. L. C. & Mensbrugghe, D. van der. Predicting Long-Term Food Demand, Cropland Use, and Prices. *Annu. Rev. Resour. Econ.* **8**, 417–441 (2016).

46. Thompson, W. *et al.* Long-term crop productivity response and its interaction with cereal markets and energy prices. *Food Policy* **84**, 1–9 (2019).

47. Peterson, W. International supply response. *Agric. Econ.* **2**, 365–374 (1988).

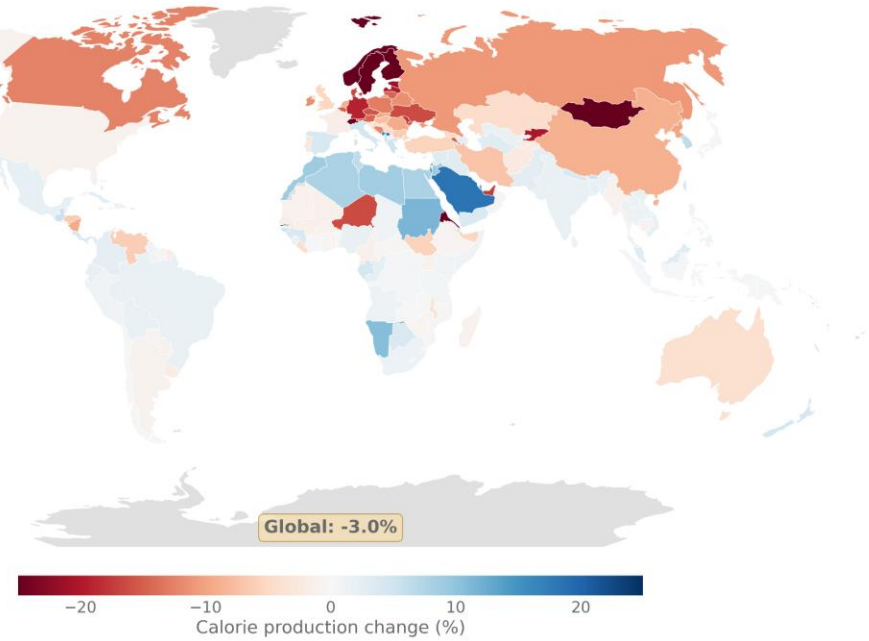
48. Bogmans, C., Pescatori, A., Petrella, I., Prifti, E. & Stuermer, M. The Power of Prices: How Fast Do Commodity Markets Adjust to Shocks? *IMF Work. Pap.* **2024**, (2024).

Extended Data

Irrigation Bounding Scenarios

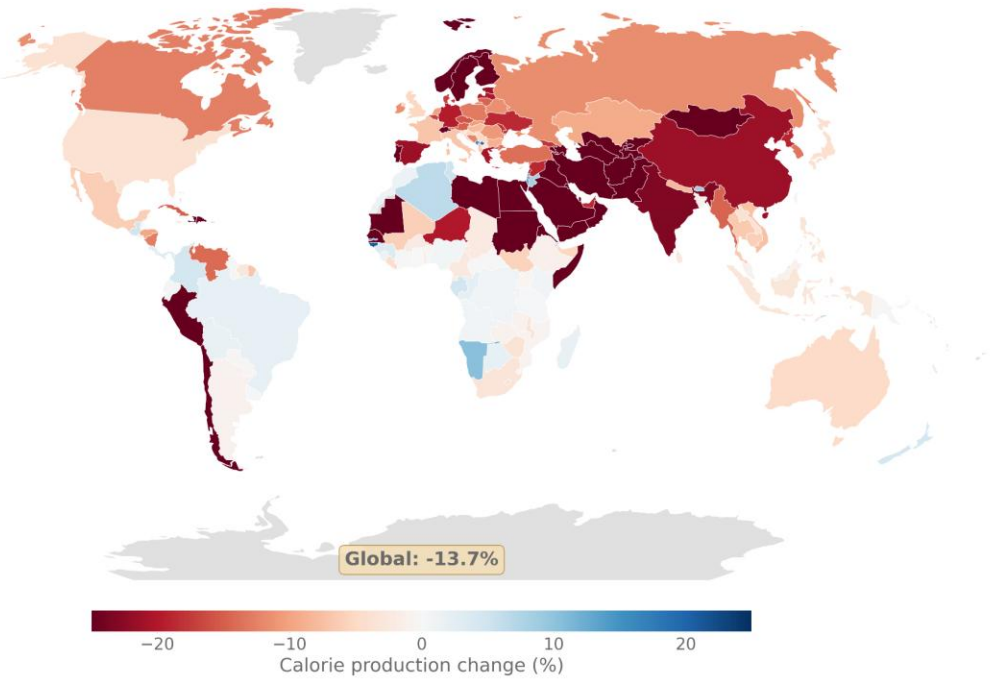
To validate the primary Precipitation-Scaled Irrigation scenario utilized in the main text, two extreme methodological bounds were established to quantify the absolute limits of the biophysical hazard. Evaluating the extreme bounds of the irrigation proxy demonstrates the critical mitigating role of global water infrastructure.

Optimistic Bound (Full Irrigation): This scenario assumes current global irrigation applications continue unabated despite the severe hydrological deficits introduced by an AMOC collapse. Under this parameter, the global caloric penalty is heavily buffered, resulting in a 3.3% structural decline.



Extended Data Figure 1: Optimistic biophysical bounds of global caloric yield anomalies under a Full Irrigation scenario. *This sensitivity analysis maps the spatial distribution of yield changes assuming all present-day irrigation applications continue unabated despite severe hydrological deficits triggered by an AMOC collapse. The buffering capacity of unconstrained global water infrastructure isolates the shock from the precipitation deficit, limiting the aggregate global caloric penalty to a 3.3% decline.*

Pessimistic Bound (No Irrigation): This scenario assumes a complete failure of all irrigation infrastructure, leaving crops entirely rainfed. While this establishes a firm lower bound, it is practically unrealistic, as a significant portion of global irrigation is drawn from deep groundwater aquifers or resilient surface water systems that would not deplete immediately upon a precipitation shock. Under this unmitigated parameter, the biophysical shock is severely compounded, driving a 13.7% absolute reduction in global baseline calories.



Extended Data Figure 2: Pessimistic biophysical bounds of global caloric yield anomalies under a No Irrigation scenario. *This sensitivity analysis demonstrates the absolute lower biophysical bounds of crop viability, assuming a complete failure of global irrigation infrastructure and transitioning all agricultural grid cells to strictly rainfed conditions. The compounding effects of the AMOC-induced thermal shock and unmitigated moisture deficits drive a severe 13.7% absolute reduction in global baseline caloric production.*

Data Availability

The HadGEM3-GC3.1-MM climate anomaly dataset utilized in this study is publicly available via Zenodo at https://zenodo.org/records/18303958.

The crop model outputs can be downloaded at https://doi.org/10.17605/OSF.IO/JB8ST.

Code Availability

The Mink global gridded crop model framework is available at: https://github.com/allfed/mink.

The complete trade model calculations can be found at: https://doi.org/10.5281/zenodo.20935272.

The partial equilibrium economic model is available at: https://osf.io/qh8zu/?view_only=37f584585957445885921cddbd2a5e78.

Acknowledgements

We thank Dr. Laura Jackson for providing the HadGEM3-GC3.1-MM climate simulation data. Thanks to Juan B. García Martínez for feedback on the manuscript.

Author Contributions

R.F. M.H. and S.B. conceptualized the study. S.B., F.U.J., M.H., R.F. and D.C.D. collaboratively designed the overarching methodology. R.F. conducted literature review, managed project administration, and wrote the original manuscript draft. S.B. executed the biophysical crop simulations. F.U.J. developed and executed the global trade network analysis. M.H. executed the

partial equilibrium economic modeling. E.C., M.S., and S.A.H. contributed to literature review. D.C.D. acquired funding and supervised the project. All authors contributed to the review and editing of the final manuscript.

Funding

This research was supported by the Alliance to Feed the Earth in Disasters (ALLFED).

Competing Interests

The authors declare no competing interests.

Corresponding Author

Rebecca Frank (rebecca@allfed.info)